JCTC Journal of Chemical Theory and Computation

Article

pubs.acs.org/JCTC

Local Excitation Approximations to Time-Dependent Density Functional Theory for Excitation Energies in Solution

Jie Liu and John M. Herbert*

Department of Chemistry and Biochemistry, The Ohio State University, Columbus, Ohio 43210, United States

Supporting Information

ABSTRACT: We derive, implement, and test three different local excitation approximations (LEAs) to time-dependent density functional theory (TDDFT) that are designed to be extremely efficient for computing excitations that are localized on a single chromophore surrounded by explicit solvent molecules. One of these approximations is equivalent to the "TDDFT for molecular interactions" [TDDFT(MI)] method that we have introduced previously, which exploits non-orthogonal, absolutely-localized molecular orbitals to approximate full TDDFT for systems consisting of multiple, weakly-coupled chromophores. Further approximations are possible when the excitation is localized on only a single subsystem and are introduced here to reduce the cost of LEA-TDDFT(MI) with respect even to TDDFT(MI). We apply these methods to compute solvatochromatic shifts for the $n \rightarrow \pi^*$ excitations in aqueous acetone and pyridine. The LEA-TDDFT(MI) method accurately reproduces the solvent-induced blue shifts in these systems, at a significant reduction in cost as compared to conventional TDDFT.

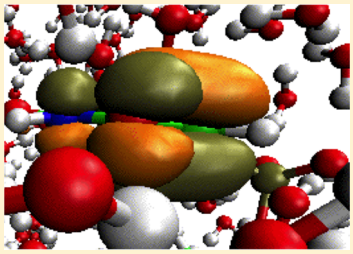

I. INTRODUCTION

Excited electronic states are crucial to understand the photophysical and photochemical process of biological and other condensed-phase chromophores,[1−5] where they are intimately influenced by the surrounding environment. The solvent effect can be divided into three parts: the solvent polarization effect, specific solute−solvent interactions such as hydrogen bonds, and the dynamic solvent effect, which means the average of the excited-state properties upon configuration sampling. All three components are indispensable in the theoretical description of solvent effects on electronically excited states.

The combined quantum mechanics/molecular mechanics (QM/MM) approach, in which the important part of the problem is treated via quantum mechanics and the remaining part via an empirical force field,[6−8] is an explicit solvation model intended to introduce the solvent polarization effect while retaining the quantum mechanics in a system small enough to attack with *ab initio* methods. If the non-covalent interactions are also characterized by the force field, then the specific solute−solvent interactions are empirically included in the QM/MM approach. However, the performance of the QM/MM approach is highly dependent upon the empirical parameters in the force field and the ground-state parameters may not be appropriate for excited states, where the larger and more polarizable wave function may simultaneously increase the attractive dispersion interaction but also magnify the Pauli repulsion, relative to the ground state.

Implicit solvent models are also popular in excited-state QM calculations, wherein the solvent is described as a structureless dielectric medium. Polarizable continuum models (PCMs) are a widely used family of implicit solvent models based upon reaction-field theory and boundary-element discretization of the solute/continuum interface.[9−15] PCMs implicitly include an average over different solvent configurations, via the medium's dielectric constant, but are not able to simulate *specific* solute−solvent interactions.

For specific solvent effects, a supermolecular approach is required, in which nearby solvent molecules are described at the QM level. The supermolecular method is able to describe highly specific solute−solvent interactions, yet at a cost that increases sharply with system size. As such, time-dependent density functional theory[16−19] (TDDFT) is the most widely used approach, as it scales no worse than $O(N^4)$ with system size, and better with density fitting.[20] In order to include the dynamic effect of solvent, however, configuration sampling should be carried out via molecular dynamics (MD) simulations. Thus, the problem grows from a single calculation on a solute molecule to hundreds of calculations on the supermolecular solute−solvent system.

In an effort to reduce the computational scaling of TDDFT without sacrificing accuracy, we recently introduced an approximation to linear-response TDDFT that is based on localized, non-orthogonal molecular orbitals,[21] which omits the explicit charge-transfer (CT) terms from the TDDFT working equations and thus confines the excitations within monomer units. We called this method TDDFT(MI), where the "MI" ("molecular interactions") indicates that the method is based on absolutely-localized molecular orbitals (ALMOs), as in the self-consistent field (SCF) for molecular interactions [SCF(MI)] method of Head-Gordon and co-workers.[22,23] TDDFT(MI) is a good method for systems of multiple, weakly-coupled chromophores, and in this context it can describe even

Received: August 28, 2015
Published: December 1, 2015

DOI: 10.1021/acs.jctc.5b00828
J. Chem. Theory Comput. 2016, 12, 157−166

delocalized excitations to an accuracy of 0.2−0.3 eV with respect to full linear-response TDDFT.[21]

A specific class of problems for which one might wish to use a localized version of TDDFT is to study excitation energies of a single chromophore in solution, wherein a significant number of explicit solvent molecules are treated quantum-mechanically. TDDFT(MI) works especially well in this case, with an accuracy of ∼0.1 eV with respect to full TDDFT,[21] but without the spurious CT states that often arise in systems of this type,[24−26] a problem that is not solved, in a fully satisfactory way, simply by using range-separated hybrid functionals.[27] For this particular class of problems, further approximations to TDDFT are possible that will reduce the cost even more. Here, we will introduce a local excitation approximation (LEA) to TDDFT(MI) in which all of the Coulomb and exchange couplings between the solvent molecules and the solute molecule (chromophore) are neglected. We call this method LEA-TDDFT(MI), and compared with our original TDDFT(MI) approach it has three attractive features.

(1) Calculations can be performed on very large systems, since the time-consuming TDDFT part is restricted in a small central region of the whole system, i.e., the chromophore only. The QM part is restricted in an active region, as indicated in Figure 1,

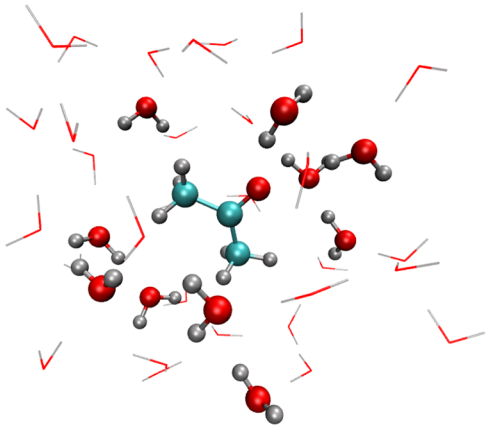

Figure 1. Schematic picture for an acetone/water cluster. The ball-and-stick molecules constitute the QM region.

which simulates both specific solvent effects (such as hydrogen bonds) and non-specific effects (such as polarization). The MM part allows a large number of solvent molecules to be explicitly included, which describes the long-range electrostatic interactions.

(2) Excited-state calculations restricted to the central system allow an easy confirmation of the target state in comparison with the supermolecular approach. Especially in TDDFT calculations, it avoids unphysical results introduced by mixing with spurious, low-energy CT states.[24−26]

(3) In comparison with other local excitation schemes,[33−36] the localized molecular orbitals on the solute molecule that are used in this work are well-defined and computed from SCF calculations.

The aim of this work is to propose an efficient LEA to time-dependent density functional theory and to compare it to our original TDDFT(MI) approach.[21] In addition, we will test a frozen molecular orbital embedding method, where the effect of the solvent molecules is included only insofar as they modify the chromophore's MOs and orbital energies. All three of these approximate TDDFT approaches will be applied to investigate solvatochromatic shifts by performing a statistical average of TDDFT calculations for configurations extracted from MD simulations. The solvatochromatic shift in the $n \rightarrow \pi^*$ excitation for acetone in aqueous solution has become a standard test case for evaluating the performance of theoretical approaches for describing solvent effects on excitation energies[37,38] and will be studied here. Reliable reference data are available since many experimental[39−41] and theoretical studies[36,42−47] have been carried out for this system. The experimental shift is 0.19−0.21 eV.[39−41] As a second test, we will consider pyridine in aqueous solution. Although no experimental data on the $n \rightarrow \pi^*$ excitation are available for this system, the shift has been estimated theoretically to lie in the range 0.25−0.37 eV.[48] We will demonstrate that the present methodology is capable of reproducing these shifts.

II. THEORY

A. TDDFT Based on Non-orthogonal MOs. The non-Hermitian linear-response TDDFT eigenvalue equation in a basis of non-orthogonal MOs is[21]

$$\begin{pmatrix} \mathbf{A} & \mathbf{B} \\ \mathbf{B} & \mathbf{A} \end{pmatrix}\begin{pmatrix} \mathbf{X} \\ \mathbf{Y} \end{pmatrix} = \omega \begin{pmatrix} \mathbf{\Delta} & \mathbf{0} \\ \mathbf{0} & -\mathbf{\Delta} \end{pmatrix}\begin{pmatrix} \mathbf{X} \\ \mathbf{Y} \end{pmatrix} \tag{1}$$

where the matrices **A**, **B**, and **Δ** are defined as

$$A_{ai\sigma,bj\sigma'} = F_{ab}S_{ij}\delta_{\sigma\sigma'} - F_{ij}S_{ab}\delta_{\sigma\sigma'} + (a_\sigma i_\sigma|b_{\sigma'}j_{\sigma'}) - C_x\delta_{\sigma\sigma'}(a_\sigma b_\sigma|i_\sigma j_{\sigma'}) + f^{xc}_{ai\sigma,bj\sigma'} \tag{2}$$

$$B_{ai\sigma,bj\sigma'} = (a_\sigma i_\sigma|b_{\sigma'}j_{\sigma'}) - C_x\delta_{\sigma\sigma'}(a_\sigma j_\sigma|b_{\sigma'}i_{\sigma'}) + f^{xc}_{ai\sigma,bj\sigma'} \tag{3}$$

$$\Delta_{ai\sigma,bj\sigma'} = S_{ab}S_{ij}\delta_{\sigma\sigma'} \tag{4}$$

Two-electron integrals are expressed in Mulliken notation, and C_x is the coefficient of Hartree−Fock exchange, in the case of a hybrid functional. Indices i, j, ... label occupied MOs; a, b, ... label virtual MOs; and p, q, ... label arbitrary MOs.

The general MOs ϕ_p are defined as

$$\phi_i = \sum_j \tilde{\phi}_j S_{ij} \tag{5}$$

$$\phi_a = (1 - \hat{\rho}_0)\tilde{\phi}_a \tag{6}$$

where $\tilde{\phi}_p$ are non-orthogonal MOs, which in this work will be ALMOs.[22,23] The quantity

$$\hat{\rho}_0 = \sum_i |\phi_i\rangle\langle\tilde{\phi}_i| \tag{7}$$

is the ground-state density operator, and **S** is the overlap matrix among the general MOs:

$$S_{pq} = \langle\phi_p|\phi_q\rangle = (\tilde{\mathbf{S}}^{-1})_{pq} \tag{8}$$

where $\tilde{\mathbf{S}}$ is the overlap matrix among the non-orthogonal MOs. The Fock matrix **F** has elements

$$F_{pq\sigma} = -\frac{1}{2}\langle\phi_{p\sigma}|\hat{\nabla}^2|\phi_{q\sigma}\rangle + V_{ext,pq\sigma} + V^{xc}_{pq\sigma} + \sum_{i,\sigma'}\left[(p_\sigma q_\sigma|i_{\sigma'}i_{\sigma'}) - C_x(p_\sigma i_\sigma|q_{\sigma'}i_{\sigma'})\delta_{\sigma\sigma'}\right] \tag{9}$$

The quantity

DOI: 10.1021/acs.jctc.5b00828
J. Chem. Theory Comput. 2016, 12, 157−166

$$V^{xc}(\mathbf{r}) = \frac{\delta E^{xc}}{\delta \rho(\mathbf{r})} \tag{10}$$

is the exchange-correlation potential, and the exchange-correlation kernel is defined as

$$f^{xc}(\mathbf{r}_1, \mathbf{r}_2) = \frac{\delta E^{xc}}{\delta \rho(\mathbf{r}_1)\, \delta \rho(\mathbf{r}_2)} \tag{11}$$

B. Local Excitation Approximations. In the case of weakly interacting molecular units, only local electronic excitations within the central subsystem (chromophore) are of interest. The TDDFT working equation on the central subsystem can be approximated as

$$\begin{pmatrix} \mathbf{A}_L & \mathbf{B}_L \\ \mathbf{B}_L & \mathbf{A}_L \end{pmatrix} \begin{pmatrix} \mathbf{X}_L \\ \mathbf{Y}_L \end{pmatrix} = \omega \begin{pmatrix} \mathbf{\Delta}_L & \mathbf{0} \\ \mathbf{0} & -\mathbf{\Delta}_L \end{pmatrix} \begin{pmatrix} \mathbf{X}_L \\ \mathbf{Y}_L \end{pmatrix} \tag{12}$$

where the matrices $\mathbf{A}_L$, $\mathbf{B}_L$, and $\mathbf{\Delta}_L$ are the local sub-blocks of the matrices $\mathbf{A}$, $\mathbf{B}$, and $\mathbf{\Delta}$ in eq 1, i.e., the blocks where indices a, i, b, and j all belong to the chromophore. We will refer to eq 12 as the LEA-TDDFT(MI) working equation. In comparison with the standard TDDFT method, the size of the $\mathbf{A}_L$, $\mathbf{B}_L$, and $\mathbf{\Delta}_L$ matrices is significantly reduced if the size of the chromophore is small compared to the size of the entire system. Furthermore, insofar as the central subsystem (chromophore) is fixed, the size of $\mathbf{A}_L$, $\mathbf{B}_L$, and $\mathbf{\Delta}_L$ remains the same as the supersystem grows larger, e.g., due to the addition of explicit solvent molecules. Environmental effects on electronic excitation of the chromophore can therefore tractably be included by making the supersystem as large as possible.

Equation 12 involves an overlap matrix among general MOs so that the solution of this equation is a bit different as compared to standard linear-response TDDFT. Below, we introduce three schemes for the LEA based on eq 12. For easy reference, these three approaches are then summarized in section IID.

1. Frozen MO Embedding. Sneskov et al.[47] have shown that, for acetone, the main effect of solvent polarization is captured already in the description of the ground state, with only minor contributions to the excited state. Besley et al.[49] explicitly take the full system into account during the SCF calculation and restrict the active molecular orbitals for the TDDFT calculation to those orbitals significantly localized on the solute molecule, introducing what is effectively an active space approximation to linear-response TDDFT. A comparable approximation in the present framework is to let the non-orthogonal MOs ϕ_p in eq 12 be ALMOs, which we denote by $\tilde{\phi}_p$. Since the ALMOs satisfy $\langle \tilde{\phi}_p | \tilde{\phi}_q \rangle = \delta_{pq}$ on the solute molecule, the sub-block of the overlap matrix in eq 12 is a unit matrix. In this approach, solvent polarization arises solely due to the change of the MOs and orbital energies on the chromophore due to the presence of the solvent molecules, which is in some sense a "zeroth-order" approximation to full TDDFT. For that reason, we refer to this scheme as "LEA0".

2. Non-orthogonal Linear-Response TDDFT Method. Actually the difference between eq 12 and standard TDDFT lies only in the overlap matrix, which indicates that it is possible to transform eq 12 into the standard TDDFT working equation. The first step is a symmetric orthogonalization procedure to obtain orthogonal molecular orbitals $\phi_p^{\perp}$ that are defined as

$$\phi_i^{\perp} = \sum_j \phi_j (\mathbf{S}^{-1/2})_{ij} \tag{13a}$$

$$\phi_a^{\perp} = \sum_b \phi_a (\mathbf{S}^{-1/2})_{ab} \tag{13b}$$

In this orthogonal representation, the matrices $\mathbf{A}$, $\mathbf{B}$, and $\mathbf{\Delta}$ have elements

$$A^{\perp}_{ai\sigma,bj\sigma'} = F^{\perp}_{ab}\delta_{ij}\delta_{\sigma\sigma'} - F^{\perp}_{ij}\delta_{ab}\delta_{\sigma\sigma'} + (a_\sigma i_\sigma | b_{\sigma'} j_{\sigma'})^{\perp} - C_x \delta_{\sigma\sigma'} (a_\sigma b_\sigma | i_{\sigma'} j_{\sigma'})^{\perp} + f^{xc,\perp}_{ai\sigma,bj\sigma'} \tag{14}$$

$$B^{\perp}_{ai\sigma,bj\sigma'} = (a_\sigma i_\sigma | b_{\sigma'} j_{\sigma'})^{\perp} - C_x \delta_{\sigma\sigma'} (a_\sigma j_\sigma | b_{\sigma'} i_{\sigma'})^{\perp} + f^{xc,\perp}_{ai\sigma,bj\sigma'} \tag{15}$$

$$\Delta^{\perp}_{ai\sigma,bj\sigma'} = \delta_{ij}\delta_{ab}\delta_{\sigma\sigma'} \tag{16}$$

As discussed by Miura and Aoki,[34] the dense structure of the Fock matrix, which corresponds to the non-diagonal structure of matrix $\mathbf{F}^{\perp}$ in eq 14, may lead to slow convergence of Davidson's iterative diagonalization procedure.[50,51] In order to eliminate the off-diagonal matrix element of the Fock matrix $\mathbf{F}^{\perp}$, one effective method is to introduce a set of quasi-canonical MOs (QCMOs), ϕ_p^{Q}:

$$\phi_i^{Q} = \sum_j U_{ij} \phi_j^{\perp} \tag{17a}$$

$$\phi_a^{Q} = \sum_b V_{ab} \phi_b^{\perp} \tag{17b}$$

The transformation to the QCMO representation satisfies the conditions

$$F^{Q}_{ij} = \sum_{kl} U_{ik} F^{\perp}_{kl} U_{lj} = \varepsilon_i \delta_{ij} \tag{18a}$$

$$F^{Q}_{ab} = \sum_{cd} V_{ac} F^{\perp}_{cd} V_{db} = \varepsilon_a \delta_{ab} \tag{18b}$$

With these QCMOs, eq 12 has exactly the same form as the standard TDDFT working equation,

$$A^{Q}_{ai\sigma,bj\sigma'} = (\varepsilon_a - \varepsilon_i)\delta_{ab}\delta_{ij}\delta_{\sigma\sigma'} + (a_\sigma i_\sigma | b_{\sigma'} j_{\sigma'})^{Q} - C_x \delta_{\sigma\sigma'} (a_\sigma b_\sigma | i_{\sigma'} j_{\sigma'})^{Q} + f^{xc,Q}_{ai\sigma,bj\sigma'} \tag{19}$$

$$B^{Q}_{ai\sigma,bj\sigma'} = (a_\sigma i_\sigma | b_{\sigma'} j_{\sigma'})^{Q} - C_x \delta_{\sigma\sigma'} (a_\sigma j_\sigma | b_{\sigma'} i_{\sigma'})^{Q} + f^{xc,Q}_{ai\sigma,bj\sigma'} \tag{20}$$

$$\Delta^{Q}_{ai\sigma,bj\sigma'} = \delta_{ij}\delta_{ab}\delta_{\sigma\sigma'} \tag{21}$$

We will refer to this particular LEA-TDDFT(MI) scheme as "LEA-Q".

3. TDDFT(MI) Method. As discussed in our previous work,[21] the TDDFT(MI) working equation can be expanded within the monomer excited basis states,

$$\frac{1}{2}\sum_n [(\mathbf{X}' + \mathbf{Y}')^{\dagger}_m (\mathbf{A}_L + \mathbf{B}_L)(\mathbf{X}' + \mathbf{Y}')_n + (\mathbf{X}' - \mathbf{Y}')^{\dagger}_m (\mathbf{A}_L - \mathbf{B}_L)(\mathbf{X}' - \mathbf{Y}')_n] U_n = \omega \sum_n [(\mathbf{X}'_m)^{\dagger} \mathbf{\Delta}_L \mathbf{X}'_n - (\mathbf{Y}'_m)^{\dagger} \mathbf{\Delta}_L \mathbf{Y}'_n] U_n \tag{22}$$

DOI: 10.1021/acs.jctc.5b00828
J. Chem. Theory Comput. 2016, 12, 157−166

The subscript n indicates the nth excited state of the central subsystem, and $|\mathbf{X}',\mathbf{Y}'\rangle$ is a transition density for the gas-phase calculation. The amplitudes $\mathbf{X}$ and $\mathbf{Y}$ can be expressed as

$$\mathbf{X} = \sum_m U_m \mathbf{X}'_m \tag{23a}$$

$$\mathbf{Y} = \sum_m U_m \mathbf{Y}'_m \tag{23b}$$

where $\mathbf{U}$ is obtained by diagonalizing eq 22. In contrast to the LEA0 approach, here the overlap effect between the chromophore subsystem and the solvent molecules has been included, and herein we call this approach LEAc. It is a localized version (in the sense that $|\mathbf{X}',\mathbf{Y}'\rangle$ is computed only for the chromophore) of the TDDFT(MI) method introduced in ref 21.

C. Absolutely Localized MOs. The definition of a localized MO is central to the success of implementing the various LEAs introduced here. In comparison with the localized MOs proposed in other LEA-TDDFT methods,[33−36] the ALMOs used in this work are well-defined and *absolutely* localized, in the sense that only AO basis functions centered on a given subsystem are allowed to contribute to that subsystem's MOs. The ALMOs are largely free of the "orthogonalization tails" that typically appear upon orbital localization. Several versions of the SCF(MI) procedure to compute ALMOs have been introduced; we used Stoll's method,[52] as implemented by Khaliullin et al.[22,23]

Although the ALMOs are absolutely localized, the general MOs and the QCMOs, which are used to compute Fock-like matrices, are delocalized over the whole system. The construction of these Fock-like matrices scales as $O(N^4)$ with system size N, or $O(N^3)$ with the density fitting,[20] although integral screening often reduces this to $O(N^2)$ in large systems. Construction of these Fock-like matrices will become the bottleneck in solving the LEA-TDDFT(MI) eigenvalue equation. In the case of weakly-interacting subsystems, however, the coupling between the central chromophore and the environment is very small, meaning that the orbitals of interest remain localized. Therefore, it is feasible to re-define a set of ALMOs φ'_p to approximate the general MOs in the LEAc method or to approximate the QCMOs in the LEA-Q method.[36]

Expanding the MOs φ'_p in subsets of atomic orbitals χ_μ centered on the central subsystem A, we have

$$\varphi'_i = \sum_{\mu,i\in A} C'_{\mu i}\chi_\mu \tag{24}$$

The expansion coefficients can be computed by minimizing the functional

$$d = \int [\varphi'_i(\mathbf{r}) - \phi_i(\mathbf{r})]^2 \, \mathrm{d}\mathbf{r} \tag{25}$$

This minimization amounts to the solution of linear equations

$$\sum_{\nu,i\in A} S_{\mu\nu}C'_{\nu,i} = \langle\phi_i|\chi_\mu\rangle \tag{26}$$

The procedure for the QCMOs (ϕ_i^{Q}) is the same. The more diffuse the basis functions are, the more solvent molecules the general MOs or QCMOs spread over, making it necessary to adopt a larger subset of atomic orbitals surrounding the central subsystem in the procedure above. Of course, if the central subsystem is large enough, then the effect of the diffuse basis functions will be insignificant since we focus only on excitations of the central subsystem.

D. Overview of the LEA Schemes. Three different LEA schemes have been introduced above: LEA0, LEA-Q, and LEAc, the latter being a localized version of the TDDFT(MI) method of ref 21. All three schemes require solution of TDDFT equations (i.e., Casida equations[17]) whose dimension is no larger than that required for a TDDFT calculation performed on the chromophore only.

At one end of the accuracy spectrum of these three methods is LEA0, in which we simply solve eq 12 in a basis of ALMOs for the chromophore. In this approach, the entirety of the solvent effect lies in how the chromophore's ALMOs are affected by the presence of the environment during the SCF(MI) iterations. At the other end of the spectrum of accuracy is the original TDDFT(MI) method,[21] in which we compute a basis of monomer excited states that are then coupled together via eq 22 in order to obtain excited states of the supersystem. As shown in previous work,[21] this method works even in cases where the excitation is delocalized across more than one chromophore unit.

However, in cases where the excitation *is* localized and weakly coupled to the excited states of the solvent molecules, the LEAc and LEA-Q methods reserve the overlap effect but discard the excited-state couplings between the solvent molecules and the solute molecules, which will be shown below to work quite well. LEAc is a version of TDDFT(MI) in which eq 22 is solved using a transition density $|\mathbf{X}',\mathbf{Y}'\rangle$ for the chromophore only; hence excited-state calculations on the solvent molecules are not required. Both LEAc and LEA-Q start from ALMOs computed for the chromophore, but in the latter case we subject these orbitals to a number of transformations leading ultimately to a version of the Casida equations (eq 12) expressed in a localized version of the QCMO basis (eqs 19−21), which is then solved via Davidson iteration. For clarity, these specific transformations are discussed in the Appendix.

III. RESULTS AND DISCUSSION

The LEA0, LEA-Q, and LEAc methods have been implemented in a locally modified version of Q-Chem.[53] Stoll's SCF(MI) method,[52] as implemented in Q-Chem by Khaliullin et al.,[22] is used to compute the ground-state ALMOs.

Table 1. Deviations in the $^1n\pi^*$ Excitation Energy of Aqueous Acetone for LEA-TDDFT(MI) Methods[a]

		Mean signed error (eV)			
config	excitation energy (eV)	LEA0	LEA-Q(0)	LEA-Q(2)	LEAc(0)
1	4.581	0.027	0.009	0.009	0.009
2	4.404	0.042	0.033	0.007	0.030
3	4.371	0.016	0.001	0.009	0.001
4	4.292	0.077	0.041	0.006	0.039
5	4.485	0.063	0.047	0.019	0.046
6	4.396	0.040	0.027	0.012	0.027
7	4.740	0.033	−0.012	0.003	−0.013
8	4.261	0.049	0.024	0.035	0.020
9	4.498	0.082	0.040	0.027	0.033
10	4.421	0.062	0.036	0.019	0.034
MAE		0.049	0.027	0.015	0.025

[a]With respect to a full TDDFT calculation, PBE0/6-311G* level.

A total of 600 configurations for aqueous acetone and aqueous pyridine were extracted from a molecular dynamics (MD) simulation run at ambient density and T = 298 K, as described in the Supporting Information. These simulations employed the

DOI: 10.1021/acs.jctc.5b00828
J. Chem. Theory Comput. 2016, 12, 157−166

Table 2. CPU Time (in Seconds) and Number of Iterations (in Parentheses) To Compute the $^1n\pi^*$ Excitation Energy of Acetone in Clusters of 13−16 Water Molecules[a]

	LEAc			LEA-Q			TDDFT			
config	SCF(MI)	TDDFT	total	SCF(MI)	TDDFT	total	SCF	TDDFT	total	speed-up[b]
1	129 (14)	175 (14)	399	127 (14)	150 (10)	346	161 (15)	1155 (12)	1067	3.1
2	202 (14)	202 (16)	519	198 (14)	179 (13)	464	252 (15)	1454 (14)	1426	3.1
3	229 (13)	162 (11)	516	229 (13)	183 (15)	508	293 (14)	1277 (11)	1768	3.5
4	217 (14)	168 (13)	497	213 (14)	162 (12)	466	267 (15)	1588 (9)	1565	3.4
5	219 (14)	147 (10)	477	212 (14)	152 (10)	447	256 (14)	1514 (15)	1858	4.2
6	220 (14)	171 (12)	506	221 (14)	142 (9)	450	265 (14)	1322 (16)	1794	4.0
7	208 (14)	160 (11)	477	203 (14)	164 (11)	447	243 (14)	2213 (11)	1580	3.5
8	358 (15)	173 (13)	672	357 (15)	212 (17)	681	412 (14)	1176 (12)	2643	3.9
9	254 (15)	195 (14)	571	252 (15)	179 (13)	520	304 (15)	1131 (8)	1496	2.9
10	215 (14)	180 (13)	510	212 (14)	170 (12)	468	271 (15)	1089 (9)	1420	3.0

[a]PBE0/6-311G* level. [b]Total TDDFT time divided by the total LEA-Q time.

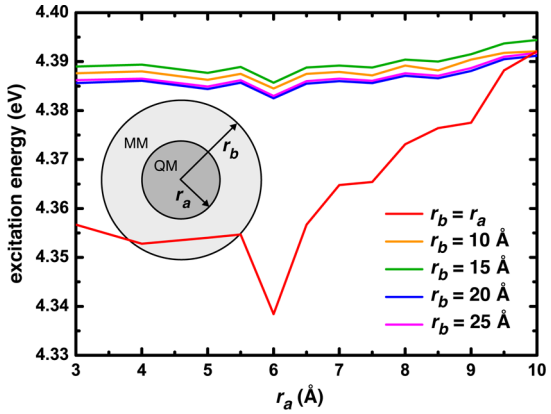

Figure 2. TD-PBE0/6-311G* excitation energies for the $n \rightarrow \pi^*$ transition of aqueous acetone, as a function of the size of the QM region (r_a) and the total QM + MM region (r_b).

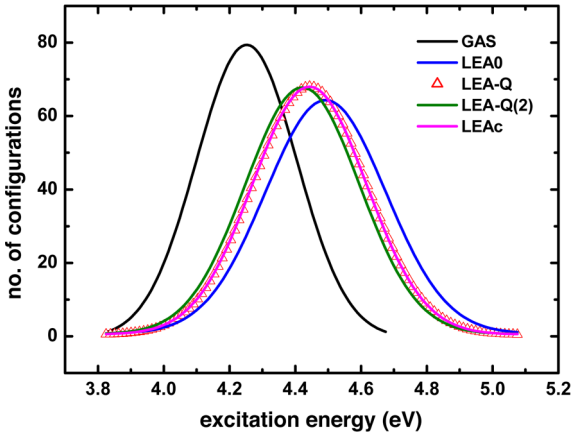

Figure 3. Calculated $n \rightarrow \pi^*$ excitation energies of aqueous acetone at the TD-PBE0/6-311++G* level with different LEA-TDDFT(MI) methods. The curves are Gaussian fits to the statistical distributions of excitation energies over 600 individual configurations. The LEA-Q and LEAc curves are essentially indistinguishable.

OPLS-AA force field[54,55] for the solute and the SPC force field[56] for water. TDDFT calculations were then performed on these solvent configurations to generate an absorption spectrum.

Denoting by r the distance between a solvent molecule and the solute, each different QM/MM method will be labeled as (r_a, r_b) where solvent molecules are included in the QM part if $r < r_a$ and

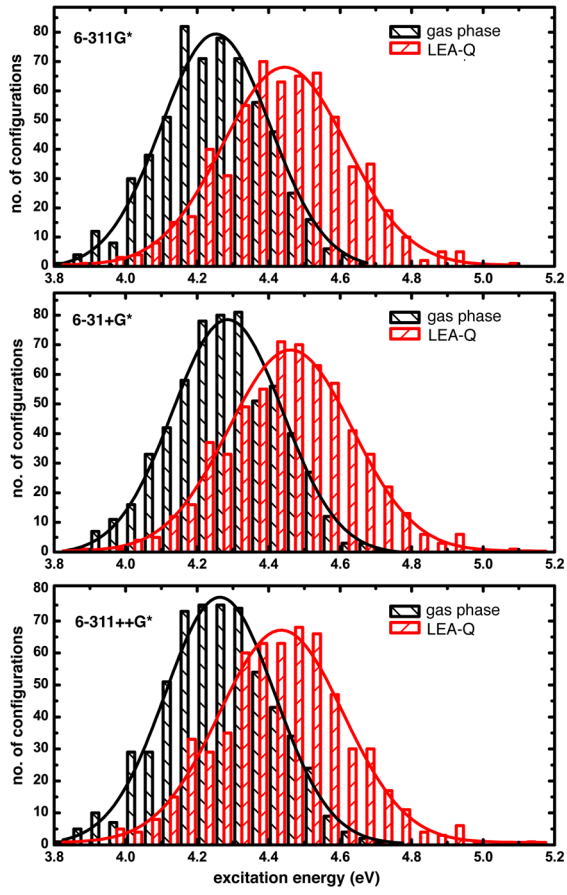

Figure 4. Calculated $n \rightarrow \pi^*$ excitation energies for aqueous acetone by at the TD-PBE0 level using various basis sets. The curves are Gaussian fits to the statistical distributions of excitation energies.

in the MM part if $r_a < r < r_b$. The quantity r_b indicates the size of the cluster that is extracted from the bulk MD simulation for the QM/MM calculation. We will also use the notation LEA0(n) to indicate a LEA0 calculation in which n water molecules are explicitly included in the solute (chromophore) subsystem; when n = 0, we will simply refer to the method as LEA0. The notations LEA-Q(n) and LEAc(n) are defined analogously.

A. Accuracy and Efficiency. In this section, all calculations are performed with the (r_a = 3 Å, r_b = 20 Å) scheme for acetone. For 10 randomly selected configurations of acetone in water, Table 1 lists the errors in the $n \rightarrow \pi^*$ excitation energy for various

DOI: 10.1021/acs.jctc.5b00828
J. Chem. Theory Comput. 2016, 12, 157−166

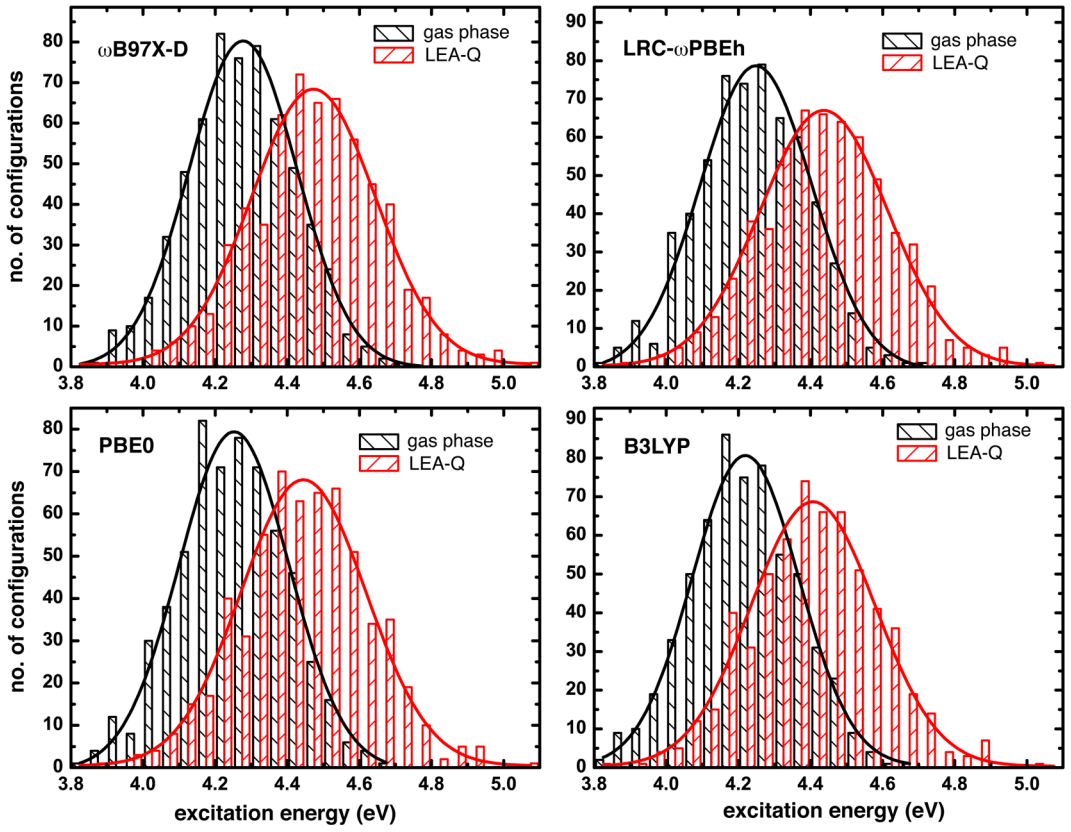

Figure 5. Calculated $n \rightarrow \pi^*$ excitation energies of aqueous acetone by TDDFT with different exchange-correlation functionals. The basis set is 6-311++G*. The curves are Gaussian fits to the statistical distributions of excitation energies.

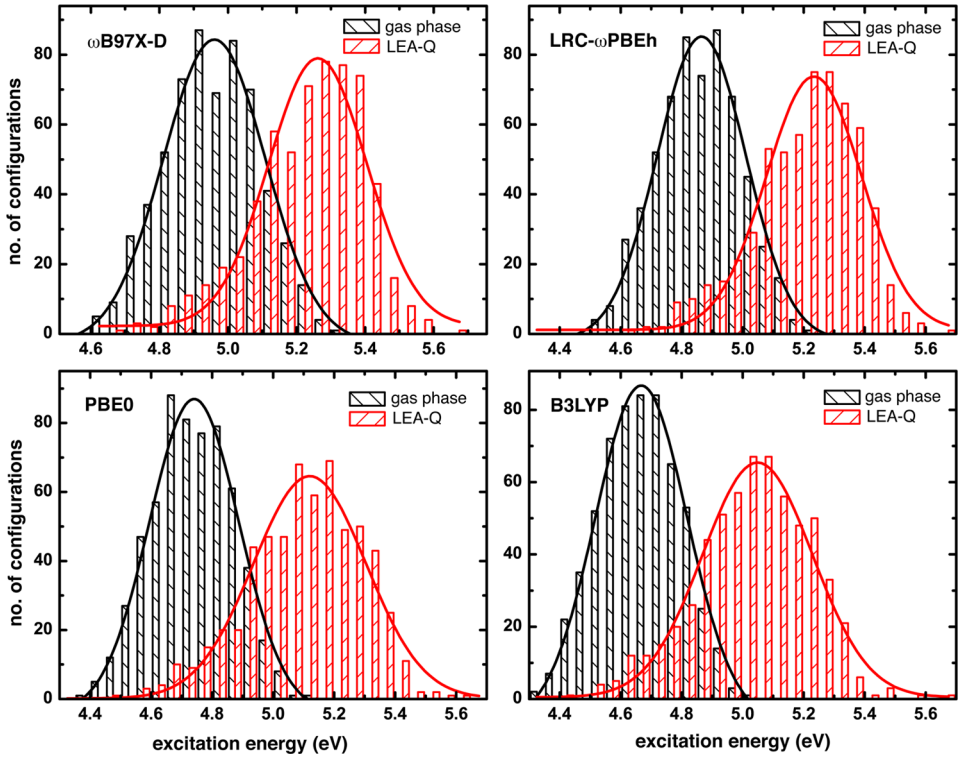

Figure 6. Calculated $n \rightarrow \pi^*$ excitation energies of aqueous pyridine by TDDFT with different exchange-correlation functionals. The basis set is 6-311++G*. The solid lines are fitted to the statistical distributions of the excitation with the Gaussian function.

LEA approximations, as compared to the full TDDFT calculation applied to the entire supersystem (explicit water molecules out to 3 Å and SPC point charges out to a distance of 20 Å from the acetone molecule). We have carefully examined the full TDDFT

DOI: 10.1021/acs.jctc.5b00828
J. Chem. Theory Comput. 2016, 12, 157−166

results in this case to ensure that we have in fact located the $^1n\pi^*$ state, rather than some spurious CT state, and the aim of these calculations is to verify whether the LEAs accurately reproduce the energy of this state, for the same functional and basis set.

Mean absolute errors (MAEs) for the LEA-Q(0) and LEA-Q(2) methods, with respect to full TDDFT, are 0.027 and 0.015 eV, respectively. Both methods agree very well with the supersystem results. It is worth mentioning, however, that it is not reasonable to consider the supersystem TDDFT calculation as a benchmark, since in many cases the TDDFT calculation predicts $n_{O(water)} \rightarrow \pi^*$ CT character, which originates from the deficiencies in the DFT methodology.[24,25] The MAE of the LEAc(0) method, 0.025 eV, is in good agreement with the LEA-Q(0) method, and the difference between these two approaches is negligible. The MAE of the LEA0(0) is larger because this approach considers the solvent effect only at the level of how the SCF(MI) procedure modulates the MOs and orbital energies of the acetone solute.

Table 2 compares timings for the LEAc, LEA-Q, and full TDDFT calculations for the same 10 configurations considered in Table 1. (These configurations contain 13−16 water molecules plus acetone.) The timings are separated into an SCF part and a TDDFT part, and we note that the (in principle identical) SCF(MI) calculations in the LEAc and LEA-Q calculations differ by a few seconds, or 1−3%, which can be taken as the intrinsic error in these timing data. Also listed in Table 2 is the number of iterations required for both the ground- and the excited-state parts of the calculation. Although the number of TDDFT (Davidson) iterations changes from method to method and from configuration to configuration, there is no clear pattern and, in particular, there is no evidence that the LEA approaches lead to a consistently greater number of either TDDFT or SCF iterations. As such, the primary figure of merit in comparing these methods is the total computer time required.

The LEAc approach is slightly slower than LEA-Q, primarily because it requires projecting eq 12 onto a subspace; see eqs 22 and 23. The LEA-Q method is found to be 3−4 times faster than full TDDFT, for these small clusters and with a moderate-sized (6-311G*) basis set; the speedup will be larger as the number of explicit solvent molecules is increased. For these relatively small systems, the SCF(MI) procedure does not afford significant speedup; hence, the SCF part of the timings is nearly the same in the LEA-Q and full TDDFT approaches, but the TDDFT time is greatly reduced for LEA-Q. As cluster size grows, the computational time required for the TDDFT part of LEA-Q changes very little so that the dominant contribution to the timing for large systems is the SCF(MI) part, which ultimately becomes faster than the full SCF procedure for large systems.[22]

B. Convergence with Respect to Cluster Size. Recent work has demonstrated that this kind of QM/MM treatment of solvatochromatic shifts sometimes converges quite slowly with respect to the number of explicit solvent molecules that are included,[26,57] an effect that is partly an artifact of spurious, low-energy CT states in the TDDFT calculations[24−26] but also arises due to orbital energies for the "edge waters" that are not indicative of the liquid-phase environment.[26] In Figure 2 we examine the convergence of the $n \rightarrow \pi^*$ transition in aqueous acetone as a function of the parameters r_a and r_b, for the LEA-Q method.

For a given value of r_a, the excitation energies for r_b = 10−25 Å lie very close to one another, meaning that the effect of long-range Coulomb interactions is nearly converged at r_b = 10 Å. The difference between r_b = 20 Å and r_b = 25 Å is <0.001 eV, for example, and MM embedding out to a radius r_b = 20 Å is thus converged for this small solute. (For r_b = 20 Å, the maximum deviation among all values r_a = 3−10 Å is <0.01 eV.) For solutes of this size, we conclude that the (r_a = 3 Å, r_b = 20 Å) QM/MM scheme offers a good balance between accuracy and efficiency.

The quality of QM/MM calculations is of course strongly dependent upon the force-field parameters, for H_2O in this case. To investigate the effect of the MM point charges, we can compare QM/MM excitation energies to those obtained when the full supersystem is described at the QM level. In other words, we can compare the (r_a = 10 Å, r_b = 10 Å) results to (r_a, r_b = 10 Å) results for various values of r_a ranging from 3.0 to 9.5 Å. The maximum deviation between these two calculations of the $n \rightarrow \pi^*$ excitation energy is <0.01 eV, meaning that the QM/MM method with SPC point charges provides an acceptable description of the long-range electrostatic interactions for aqueous acetone. By incorporating the most important (nearby) water molecules into the QM region, the effect of the force-field parameters becomes less significant.

C. Solvatochromatic Shifts. We next examine solvatochromatic shifts in aqueous acetone, in order to examine possible functional and basis-set dependence of the three LEAs. Figure 3 shows the statistical distributions of the $n \rightarrow \pi^*$ excitation energies for aqueous acetone calculated using the LEA0, LEA-Q, LEA-Q(2), and LEAc methods. As an aside, recall that the TDDFT ionization continuum starts at $-\varepsilon_{HOMO}$,[17] but for the 600 configurations considered in this section the minimum value of $-\varepsilon_{HOMO}$ is 6.4 eV, which is well off scale in Figure 3 and in each of the subsequent plotted spectra. (See the Supporting Information for minimum values of $-\varepsilon_{HOMO}$ using various functionals and basis sets.)

In the LEA0 method, the solvent effect arises exclusively from the changes in the orbitals and orbital energies that are polarized by their environment, whereas in the LEA-Q and LEAc methods there are additional solvent effects stemming from overlap interactions, and in LEA-Q(2) there are two explicit water molecules in the QM region, so that hydrogen bonding to the chromophore is treated explicitly. Average vertical $n \rightarrow \pi^*$ excitation energies, computed at the TD-PBE0/6-311++G* level for 600 individual solvent configurations are 4.49, 4.44, 4.42, and 4.44 eV for the LEA0, LEA-Q, LEA-Q(2), and LEAc methods, respectively. In comparison to the gas-phase excitation energy (4.25 eV) in gas phase, the solvatochromatic shift is 0.24 eV for the LEA0 method, 0.19 eV for the LEA-Q method, 0.17 eV for the LEA-Q(2) method, and 0.19 eV for the LEAc method. (The experimentally measured solvatochromatic shift is 0.19−0.21 eV.[39−41])

As compared to the LEA-Q method, LEA0 overestimates the solvent shift because it completely ignores the interaction of the solvent's MOs in the $n \rightarrow \pi^*$ excitation, since only the ALMOs of the acetone molecule are included in the TDDFT calculation, thus limiting the variational flexibility of the transition density. In the LEA-Q(2) approach, additional CT states involving the two explicit solvent molecules mix with the $n \rightarrow \pi^*$ excitation, leading to an underestimate of the solvent shift. There is very little difference between LEA-Q and LEAc results, meaning that the two different methods to solve eq 12 that are discussed in section IIIA are nearly the same in their accuracy, at least for this specific example.

Figure 4 shows the statistical distributions of the $n \rightarrow \pi^*$ excitation energies for acetone in aqueous solution calculated at the LEA-Q level with different basis sets. Gaussian fits to the simulated statistical distributions of excitation energies are

DOI: 10.1021/acs.jctc.5b00828
J. Chem. Theory Comput. 2016, 12, 157−166

shown as well, for both the gas-phase and the aqueous systems. Average solvatochromatic shifts are 0.17 eV for PBE0/6-311G* and 0.18 and 0.19 eV for the 6-31+G* and 6-311++G* basis sets, respectively, indicating the negligible influence of the basis set, and the values agree well (within k_BT) with the experimental shift of 0.19−0.21 eV.[39−41]

It has been noted that nuclear quantum effects can have a sizable effect on the width of a spectrum computed in this way,[58] although the study in ref 58 involves a much larger chromophore, for which vibrational effects may be expected to be more important as compared to those in acetone. That said, one important message to be taken from Figure 4 is that the computed width is not strongly dependent upon the choice of basis set, within a reasonable range of basis sets for TDDFT calculations, so that the issue does not lie with the LEA itself. Excitation energies reported at the TD-PBE0/6-311G* level in Table 1, for 10 of the 600 solvent configurations used to generate Figure 4, exhibit mean errors of only 0.03 eV with respect to full TDDFT, indicating that application of the LEA does not shift the distribution of excitation energies much at all. (Unlike the data in Table 2, however, where we have explicitly identified the $^1n\pi^*$ state for each solvent configuration, an attempt to compute spectra such as those in Figure 4 with full TDDFT would have to contend with the possibility of artifacts due to spurious CT states, which can cause spurious intensity-borrowing phenomena that affect the distribution of oscillator strengths.[25])

A previous study by Ma and Ma[59] found that predicted solvatochromatic shifts for acetone can be quite different among different exchange-correlation functionals, especially when comparing semilocal to hybrid functionals, although the differences among hybrids—comparing, e.g., B3LYP to ωB97X-D—were much smaller, and arise mostly from the differing description of charge transfer. Figure 5 shows the calculated electronic spectra for aqueous acetone using several different exchange-correlation functionals: PBE0,[60] B3LYP,[61,62] ωB97X-D,[63] and long-range corrected (LRC) ωPBEh.[64,65] Each of these functionals affords a solvatochromatic blue shift of 0.19−0.20 eV. The equivalent performance of these hybrid functionals within the LEA-TDDFT(MI) scheme suggests that, in each case, spurious charge transfer is excluded from the calculations.

Finally, we consider a second molecular example, namely, the lowest $n \rightarrow \pi^*$ transition for aqueous pyridine. Electronic spectra are plotted in Figure 6 and again represent averages over 600 individual configurations. Solvatochromatic shifts of 0.36 eV (PBE0), 0.36 eV (B3LYP), 0.32 eV (ωB97X-D), and 0.34 eV (LRC-ωPBEh) are obtained. Although experimental data for this particular solvent shift are not available, a shift of 0.25−0.37 eV has been estimated theoretically by Coutinho et al.[48] and 0.31 eV by Marenich et al.[66] The shifts that we compute with various functionals agree very well with these estimates.

IV. CONCLUSIONS

In this work, we have developed an efficient implementation of the local excitation approximation to TDDFT using absolutely localized molecular orbitals. In contrast to some other LEAs, in our approach a set of well-defined ALMOs is introduced in the SCF calculation at the very beginning. In fact, three different versions of LEA-TDDFT(MI) are introduced and tested here. These methods are intended to describe an excited state that is localized on a single chromophore but at the same time to allow the effects of a large number of solvent molecules to be included in the calculation, without the introduction of spurious chromophore-to-solvent CT states. This is accomplished via localization approximations such that the dimension of the TDDFT equations that must be solved reflects the chromophore only, and does not grow as the size of the environment increases.

In the LEA0 method, the solvent effect manifests only via the change in the MOs and orbital energies, as explicit overlap effects between the solute MOs and the solvent MOs are ignored. Such effects are included in the LEA-Q method, which is based on a quasi-canonicalization for improved performance and, for a system such as (acetone)$(H_2O)_n$ with n = 13−16, is about three times faster than conventional TDDFT, a gap that will only widen with increasing n. In fact, the time-to-solution (wall time) associated with the TDDFT part of an LEA-Q calculation is only related to the size of the chromophore, not to the number of solvent molecules. Solvent molecules are included in the ground-state SCF(MI) calculation, but for large systems an SCF(MI) calculation is significantly faster than a conventional SCF calculation,[22] and we therefore expect the LEA-Q approximation to TDDFT to be quite useful for larger systems where the inclusion of enough explicit solvent molecules to converge the solvatochromatic shift might render a conventional TDDFT calculation prohibitively expensive. In the present work, we have applied LEA-TDDFT(MI) to compute solvatochromatic shifts for the $n \rightarrow \pi^*$ excitations of acetone and pyridine in aqueous solution, obtaining shifts that are in good agreement with a variety of theoretical and experimental estimates.

On the other hand, the correct description of a state where the excitation is shared across multiple chromophores would require all of those participants to be included in the central LEA-Q or LEAc fragment, for which TDDFT equations are solved. This increases the cost and also potentially reintroduces spurious CT states. The better low-cost approach in such cases is the TDDFT(MI) method in ref 21, where the fragments are single chromophores but couplings among them are calculated (in the spirit of an exciton Hamiltonian[67,68]), which allows for the description of a delocalized excitation. We have addressed such cases using TDDFT(MI) in previous work.[21]

APPENDIX A: SUMMARY OF THE LEA-Q ALGORITHM

Here we provide a step-by-step overview of the LEA-Q version of TDDFT(MI) that is introduced here. For the purpose of this discussion, we divide the system, S, into a chromophore part (C) and an environment part (E), S = C ∪ E. TDDFT equations will be solved whose dimension reflects that of C only, but we first start with a ground-state SCF(MI) calculation for the entire system, which affords ALMOs $\tilde{\phi}_p$ for both the C and E regions. Consider an occupied ALMO centered on the chromophore,

$$\tilde{\phi}_{i\in C} = \sum_{\mu\in C} C^{C}_{\mu i}\chi_\mu \tag{A1}$$

which is a linear combination of AOs χ_μ centered in region C. In order to simplify the appearance of the TDDFT equation, in eq 5 we folded certain inverse overlap factors into the non-orthogonal MOs, which in this case we might write as

$$\phi_{i\in C} = \sum_{j\in S} \tilde{\phi}_j S^{CE}_{ij} \tag{A2}$$

where $\mathbf{S}^{CE}$ represents the overlap matrix between the chromophore and the environment orbitals. Alternatively, we could write

DOI: 10.1021/acs.jctc.5b00828
J. Chem. Theory Comput. 2016, 12, 157−166

$$\phi_{i\in C} = \sum_{M}^{\text{molecules}} \sum_{j\in M} \sum_{\mu\in M} C_{\mu j}^{M} S_{ij} \chi_{\mu} \tag{A3}$$

and this form makes it clear that even the MOs ϕ_i in the chromophore region are expanded in terms of AOs centered on molecules in the environment region ($M \notin C$). This is addressed later using a localization approximation.

At this point the ground-state calculation is complete and we have used the ALMOs to construct general MOs ϕ_i. We next discard the MOs $\phi_{i\in E}$, thereby reducing the dimension of eq 12 to that of a TDDFT calculation for the chromophore alone. We orthogonalize the general MOs in the chromophore region,

$$\phi_{i\in C}^{\perp} = \sum_{j\in C} \phi_j (\mathbf{S}_C^{-1/2})_{ij} \tag{A4}$$

where $\mathbf{S}_C$ is the overlap matrix for the chromophore-centered AOs. In an effort to accelerate convergence of the Davidson iterations, however, we quasi-canonicalize these orthogonal MOs (see eq 17):

$$\phi_{i\in C}^{Q} = \sum_{j\in C} U_{ij} \phi_j^{\perp} \tag{A5}$$

Finally, to facilitate integral screening we take the exact QCMOs in eq A5, which contain expansion coefficients on AOs centered in the environment, and re-expand them in terms of just those AOs centered on the chromophore (eq 24), with fitting coefficients $(C_{\mu i}^{C})'$ obtained from solving eq 26 that represents the best fit of $\phi_{i\in C}^{Q}$ to the chromophore-centered AO basis. Equation 12 is then solved for the chromophore excited states in this localized basis.

■ ASSOCIATED CONTENT

Supporting Information

The Supporting Information is available free of charge on the ACS Publications website at DOI: 10.1021/acs.jctc.5b00828.

Details of the MD simulations and values of ε_{HOMO} for the TDDFT calculations (PDF)

■ AUTHOR INFORMATION

Corresponding Author

*E-mail: herbert@chemistry.ohio-state.edu.

Notes

The authors declare no competing financial interest.

■ ACKNOWLEDGMENTS

This work was supported by the U.S. Department of Energy, Office of Basic Energy Sciences, Division of Chemical Sciences, Geosciences, and Biosciences under Award No. DE-SC0008550. Calculations were performed at the Ohio Supercomputer Center under Project No. PAA-0003.[69] J.M.H. is a Camille Dreyfus Teacher-Scholar.

■ REFERENCES

(1) Scholes, G. D.; Fleming, G. R.; Olaya-Castro, A.; van Grondelle, R. *Nat. Chem.* **2011**, *3*, 763−774.
(2) Hagfeldt, A.; Boschloo, G.; Sun, L.; Kloo, L.; Pettersson, H. *Chem. Rev.* **2010**, *110*, 6595−6663.
(3) van der Ende, B. M.; Aarts, L.; Meijerink, A. *Phys. Chem. Chem. Phys.* **2009**, *11*, 11081−11095.
(4) Navizet, I.; Liu, Y.-J.; Ferré, N.; Roca-Sanjuán, D.; Lindh, R. *ChemPhysChem* **2011**, *12*, 3064−3076.
(5) Brédas, J.-L.; Beljonne, D.; Coropceanu, V.; Cornil, J. *Chem. Rev.* **2004**, *104*, 4971−5004.
(6) Gao, J.; Xia, X. *Science* **1992**, *258*, 631−635.
(7) Cui, Q.; Karplus, M. *J. Chem. Phys.* **2000**, *112*, 1133−1149.
(8) Senn, H. M.; Thiel, W. *Angew. Chem., Int. Ed.* **2009**, *48*, 1198−1229.
(9) Chipman, D. M. *Theor. Chem. Acc.* **2002**, *107*, 80−89.
(10) Tomasi, J.; Mennucci, B.; Cammi, R. *Chem. Rev.* **2005**, *105*, 2999−3093.
(11) Lange, A. W.; Herbert, J. M. *Chem. Phys. Lett.* **2011**, *509*, 77−87.
(12) Mennucci, B. *WIREs Comput. Mol. Sci.* **2012**, *2*, 386−404.
(13) Liu, J.; Liang, W. *J. Chem. Phys.* **2013**, *138*, 024101.
(14) Mewes, J.-M.; You, Z.-Q.; Wormit, M.; Kriesche, T.; Herbert, J. M.; Dreuw, A. *J. Phys. Chem. A* **2015**, *119*, 5446−5464.
(15) Herbert, J. M.; Lange, A. W. In *Many-Body Effects and Electrostatics in Biomolecules*; Cui, Q., Ren, P., Meuwly, M., Eds.; Pan Stanford: Boca Raton, FL, USA, 2015; Chapter 1, pp 1−54.
(16) Gross, E.; Kohn, W. *Adv. Quantum Chem.* **1990**, *21*, 255.
(17) Casida, M. E. In *Recent Advances in Density Functional Methods*, Part I; Chong, D. P., Ed.; Recent Advances in Computational Chemistry, Vol. *I*; World Scientific: River Edge, NJ, USA, 1995; Chapter 5, pp 155−192.
(18) Furche, F.; Ahlrichs, R. *J. Chem. Phys.* **2002**, *117*, 7433−7447.
(19) Liu, J.; Liang, W. *J. Chem. Phys.* **2011**, *135*, 184111.
(20) van Gisbergen, S. J. A.; Guerra, C. F.; Baerends, E. J. *J. Comput. Chem.* **2000**, *21*, 1511−1523.
(21) Liu, J.; Herbert, J. M. *J. Chem. Phys.* **2015**, *143*, 034106.
(22) Khaliullin, R. Z.; Head-Gordon, M.; Bell, A. T. *J. Chem. Phys.* **2006**, *124*, 204105.
(23) Khaliullin, R. Z.; Cobar, E. A.; Lochan, R. C.; Bell, A. T.; Head-Gordon, M. *J. Phys. Chem. A* **2007**, *111*, 8753−8765.
(24) Neugebauer, J.; Louwerse, M. J.; Baerends, E. J.; Wesołowski, T. A. *J. Chem. Phys.* **2005**, *122*, 094115.
(25) Lange, A.; Herbert, J. M. *J. Chem. Theory Comput.* **2007**, *3*, 1680−1690.
(26) Isborn, C. M.; Mar, B. D.; Curchod, B. F. E.; Tavernelli, I.; Martínez, T. J. *J. Phys. Chem. B* **2013**, *117*, 12189−12201.
(27) Although range-separated hybrids (also known as long-range corrected functionals) go a long way toward remedying the spurious CT problem, adjustment of the range-separation parameter can have a non-trivial effect on valence excitation energies as well,[28−30] often degrading the accuracy with respect to global hybrid functionals. Moreover, the appropriate value of the range-separation parameter appears to exhibit a strong dependence on system size,[26,31,32] particularly in systems composed of a chromophore surrounded by numerous explicit solvent molecules,[26,31] which are precisely the systems of interest here.
(28) Rohrdanz, M. A.; Herbert, J. M. *J. Chem. Phys.* **2008**, *129*, 034107.
(29) Lange, A. W.; Rohrdanz, M. A.; Herbert, J. M. *J. Phys. Chem. B* **2008**, *112*, 6304−6308.
(30) Wong, B. M.; Cordaro, J. G. *J. Chem. Phys.* **2008**, *129*, 214703.
(31) Uhlig, F.; Herbert, J. M.; Coons, M. P.; Jungwirth, P. *J. Phys. Chem. A* **2014**, *118*, 7507−7515.
(32) Garrett, K.; Vazquez, X. A. S.; Egri, S. B.; Wilmer, J.; Johnson, L. E.; Robinson, B. H.; Isborn, C. M. *J. Chem. Theory Comput.* **2014**, *10*, 3821−3831.
(33) Li, Q.; Li, Q.; Shuai, Z. *Synth. Met.* **2008**, *158*, 330−335.
(34) Miura, M.; Aoki, Y. *J. Comput. Chem.* **2009**, *30*, 2213−2230.
(35) Yoshikawa, T.; Kobayashi, M.; Fujii, A.; Nakai, H. *J. Phys. Chem. B* **2013**, *117*, 5565−5573.
(36) Zhang, C.; Yuan, D.; Guo, Y.; Li, S. *J. Chem. Theory Comput.* **2014**, *10*, 5308−5317.
(37) Aidas, K.; Kongsted, J.; Osted, A.; Mikkelsen, K. V.; Christiansen, O. *J. Phys. Chem. A* **2005**, *109*, 8001−8010.
(38) Gomes, A. S. P.; Jacob, C. R. *Annu. Rep. Prog. Chem., Sect. C: Phys. Chem.* **2012**, *108*, 222−277.
(39) Porter, C. W.; Iddings, C. *J. Am. Chem. Soc.* **1926**, *48*, 40−44.
(40) Bayliss, N. S.; McRae, R. G. *J. Phys. Chem.* **1954**, *58*, 1006−1011.
(41) Bayliss, N. S.; Wills-Johnson, G. *Spectrochim Acta A* **1968**, *24*, 551−561.
(42) Gao, J. *J. Am. Chem. Soc.* **1994**, *116*, 9324−9328.

DOI: 10.1021/acs.jctc.5b00828
J. Chem. Theory Comput. 2016, 12, 157−166

(43) Cossi, M.; Barone, V. *J. Chem. Phys.* **2000**, *112*, 2427−2435.
(44) Marenich, A. V.; Cramer, C. J.; Truhlar, D. G. *J. Chem. Theory Comput.* **2010**, *6*, 2829−2844.
(45) Chipman, D. M. *J. Chem. Phys.* **2009**, *131*, 014103.
(46) Steindal, A. H.; Ruud, K.; Frediani, L.; Aidas, K.; Kongsted, J. *J. Phys. Chem. B* **2011**, *115*, 3027−3037.
(47) Sneskov, K.; Schwabe, T.; Christiansen, O.; Kongsted, J. *Phys. Chem. Chem. Phys.* **2011**, *13*, 18551−18560.
(48) Coutinho, K.; Saavedra, N.; Serrano, A.; Canuto, S. *J. Mol. Struct.: THEOCHEM* **2001**, *539*, 171−179.
(49) Besley, N. A.; Oakley, M. T.; Cowan, A. J.; Hirst, J. D. *J. Am. Chem. Soc.* **2004**, *126*, 13502−13511.
(50) Davidson, E. R. *J. Comput. Phys.* **1975**, *17*, 87−94.
(51) Stratmann, R. E.; Scuseria, G. E.; Frisch, M. J. *J. Chem. Phys.* **1998**, *109*, 8218−8224.
(52) Stoll, H.; Wagenblast, G.; Preuss, H. *Theor. Chem. Acc.* **1980**, *57*, 169−178.
(53) Shao, Y.; Gan, Z.; Epifanovsky, E.; Gilbert, A. T. B.; Wormit, M.; Kussmann, J.; Lange, A. W.; Behn, A.; Deng, J.; Feng, X.; Ghosh, D.; Goldey, M.; Horn, P. R.; Jacobson, L. D.; Kaliman, I.; Khaliullin, R. Z.; Kús, T.; Landau, A.; Liu, J.; Proynov, E. I.; Rhee, Y. M.; Richard, R. M.; Rohrdanz, M. A.; Steele, R. P.; Sundstrom, E. J.; Woodcock, H. L., III; Zimmerman, P. M.; Zuev, D.; Albrecht, B.; Alguire, E.; Austin, B.; Beran, G. J. O.; Bernard, Y. A.; Berquist, E.; Brandhorst, K.; Bravaya, K. B.; Brown, S. T.; Casanova, D.; Chang, C.-M.; Chen, Y.; Chien, S. H.; Closser, K. D.; Crittenden, D. L.; Diedenhofen, M.; DiStasio, R. A., Jr.; Do, H.; Dutoi, A. D.; Edgar, R. G.; Fatehi, S.; Fusti-Molnar, L.; Ghysels, A.; Golubeva-Zadorozhnaya, A.; Gomes, J.; Hanson-Heine, M. W. D.; Harbach, P. H. P.; Hauser, A. W.; Hohenstein, E. G.; Holden, Z. C.; Jagau, T.-C.; Ji, H.; Kaduk, B.; Khistyaev, K.; Kim, J.; Kim, J.; King, R. A.; Klunzinger, P.; Kosenkov, D.; Kowalczyk, T.; Krauter, C. M.; Lao, K. U.; Laurent, A.; Lawler, K. V.; Levchenko, S. V.; Lin, C. Y.; Liu, F.; Livshits, E.; Lochan, R. C.; Luenser, A.; Manohar, P.; Manzer, S. F.; Mao, S.-P.; Mardirossian, N.; Marenich, A. V.; Maurer, S. A.; Mayhall, N. J.; Neuscamman, E.; Oana, C. M.; Olivares-Amaya, R.; O'Neill, D. P.; Parkhill, J. A.; Perrine, T. M.; Peverati, R.; Pieniazek, P. A.; Prociuk, A.; Rehn, D. R.; Rosta, E.; Russ, N. J.; Sharada, S. M.; Sharma, S.; Small, D. W.; Sodt, A.; Stein, T.; Stück, D.; Su, Y.-C.; Thom, A. J. W.; Tsuchimochi, T.; Vanovschi, V.; Vogt, L.; Vydrov, O.; Wang, T.; Watson, M. A.; Wenzel, J.; White, A.; Williams, C. F.; Yang, J.; Yeganeh, S.; Yost, S. R.; You, Z.-Q.; Zhang, I. Y.; Zhang, X.; Zhao, Y.; Brooks, B. R.; Chan, G. K. L.; Chipman, D. M.; Cramer, C. J.; Goddard, W. A., III; Gordon, M. S.; Hehre, W. J.; Klamt, A.; Schaefer, H. F., III; Schmidt, M. W.; Sherrill, C. D.; Truhlar, D. G.; Warshel, A.; Xu, X.; Aspuru-Guzik, A.; Baer, R.; Bell, A. T.; Besley, N. A.; Chai, J.-D.; Dreuw, A.; Dunietz, B. D.; Furlani, T. R.; Gwaltney, S. R.; Hsu, C.-P.; Jung, Y.; Kong, J.; Lambrecht, D. S.; Liang, W.; Ochsenfeld, C.; Rassolov, V. A.; Slipchenko, L. V.; Subotnik, J. E.; Van Voorhis, T.; Herbert, J. M.; Krylov, A. I.; Gill, P. M. W.; Head-Gordon, M. *Mol. Phys.* **2015**, *113*, 184−215.
(54) Jorgensen, W. L.; Maxwell, D. S.; Tirado-Rives, J. *J. Am. Chem. Soc.* **1996**, *118*, 11225−11236.
(55) Kaminski, G. A.; Friesner, R. A.; Tirado-Rives, J.; Jorgensen, W. L. *J. Phys. Chem. B* **2001**, *105*, 6474−6487.
(56) Berendsen, H.; Grigera, J.; Straatsma, T. *J. Phys. Chem.* **1987**, *91*, 6269−6271.
(57) Isborn, C. M.; Luehr, N.; Ufimtsev, I. S.; Martínez, T. J. *J. Chem. Theory Comput.* **2011**, *7*, 1814−1823.
(58) Petrone, A.; Cerezo, J.; Ferrer, F. J. A.; Donati, G.; Improta, R.; Rega, N.; Santoro, F. *J. Phys. Chem. A* **2015**, *119*, 5426−5438.
(59) Ma, H.; Ma, Y. *J. Chem. Phys.* **2012**, *137*, 214504.
(60) Ernzerhof, M.; Scuseria, G. E. *J. Chem. Phys.* **1999**, *110*, 5029−5036.
(61) Becke, A. D. *J. Chem. Phys.* **1993**, *98*, 5648−5652.
(62) Lee, C.; Yang, W.; Parr, R. G. *Phys. Rev. B: Condens. Matter Mater. Phys.* **1988**, *37*, 785−789.
(63) Chai, J.-D.; Head-Gordon, M. *Phys. Chem. Chem. Phys.* **2008**, *10*, 6615−6620.
(64) Rohrdanz, M. A.; Martins, K. M.; Herbert, J. M. *J. Chem. Phys.* **2009**, *130*, 054112.
(65) Lange, A. W.; Herbert, J. M. *J. Am. Chem. Soc.* **2009**, *131*, 3913−3922.
(66) Marenich, A. V.; Cramer, C. J.; Truhlar, D. G.; Guido, C. A.; Mennucci, B.; Scalmani, G.; Frisch, M. J. *Chem. Sci.* **2011**, *2*, 2143−2161.
(67) Morrison, A. F.; You, Z.-Q.; Herbert, J. M. *J. Chem. Theory Comput.* **2014**, *10*, 5366−5376.
(68) Morrison, A. F.; Herbert, J. M. *J. Phys. Chem. Lett.* **2015**, *6*, 4390−4396.
(69) Ohio Supercomputer Center, http://osc.edu/ark:/19495/f5s1ph73. (Accessed Oct. 31, 2015.).

DOI: 10.1021/acs.jctc.5b00828
J. Chem. Theory Comput. 2016, 12, 157−166